Source Localization with Overlapping CW Intercepts using Multipath Modeling.

P. Blanc–Benon

Thomson-Sintra ASM, BP.157, 06903 Sophia-Antipolis Cedex, France

ABSTRACT

This paper addresses the problem of passively locating a CW pulse emitter without *a priori* information concerning the pulse duration or the number of overlapping paths being intercepted. It differs from a previous approach by Manickam [1], since it consists on jump online detections, with a single path being concerned each time. Basically, the method relies on a non-linear ML estimation of the sinusoid parameters and a jump detector based on forward-backward estimation residuals to compute the individual times of beginning/ending for each path. Using the sound speed profile, a non-linear (NL) least-squares fit between the measured time-delays and the guessed ones enables to locate the source in both range and depth. Monte-Carlo simulation in a deep Mediterranean like channel demonstrates the capability of the method for various signal to noise ratio. The Cramer-Rao bounds of the range–depth estimation are computed by using an analytic modelization of the ray propagation. At last, a 1-hour recorded signal experiment proves the at-sea efficiency of the method for a source located in the 20-30 km ranges of the deep Mediterranean channel.

1 PROBLEM STATEMENT AND ASSUMPTIONS

Underwater acoustics is frequently concerned with locating an active sonar by means of a passive sonar. The major difficulties of such a problem are:

- the energy received by the passive sonar is naturally sparse in time; often a few samples are available, from which the sonar system has to decide the position of the emitter,
- the parameter estimation procedure (to extract time-delay information) is difficult when the multipath effect is dominant: the pulse replicas overlap each other and need to be identified (which ray path is present).

Here we suppose that the intercepts are overlapping CW pulses; different methods should be applied for other classes of pulses like FM, Costas, PSK/FSK ... .

Considering an active sonar which emits a CW signal named $s(t)$ through a propagation channel (Fig. 1), the received signal can be expressed as

$$y(t) = \sum_{l=1}^{M} \alpha_l s(t-\tau_l) + w(t) \qquad (1)$$

where the attenuations α_l, the delays τ_l, and the number of paths M are depending on the channel, and $w(t)$ is a process noise assumed to be gaussian, stationary and zero–mean. From this basis, the problem is now to localize the emitter in range and depth, no matter the bearing is.

The assumptions we made are related to the knowledge of first the pulse class (here a sinusoid CW), second the sound speed profile (SSP) characterizing the medium, and finally ownship depth.

2 MODEL EQUATIONS AND PARAMETER ESTIMATION

The received signal is described by eq. (1) and the model for the input signal is simply:

$$s(t) = a\sin(2\pi f_0 t + \phi) \qquad (2)$$

ϕ being the unknown phase at the initial time. As an example, Fig. 2 presents a view of a simulated signal corresponding to a received pulse. Clearly, the entire signal is composed of SOFAR [2] replicas (that is paths with no interface interaction either surface or bottom), then in time, SRBR1 paths (a single bottom reflection and 0 up to 2 surface reflections), and finally SRBR2 paths; the others are not detected.

Taking into account the CW model, the objective is to estimate the number of replicas M and their relative time–delays from the first one, then to estimate the emitter location. To do so, a 4-step procedure is designed.

Step 1: CW pulse parameter estimation A great number of methods have been proposed to estimate sinusoid parameters [3]. Here we present rapidly a NL regression based solution using a sliding window which length is equal to N time samples. First, we estimate the frequency of the pulse, by considering the pseudo-measurement Ψ associated with the original measurement eq. (2) without noise:

$$\Psi \cdot s_{i-1} = s_i + s_{i-2} \quad (3)$$

$$\Psi \stackrel{\text{def}}{=} 2\cos 2\pi f_0 T \quad (4)$$

T being the sampling period. Stacking the noisy measurements $y_i = s_i + w_i$ (recall a single path is assumed present during NT) in a column vector for both sides of eq. (3), we get

$$Z = Y\Psi + W \quad (5)$$

with $Y = \text{col}_{i=2,N-1}\{y_i\}$, $Z = \text{col}_{i=3,N}\{y_i + y_{i-2}\}$, and $W = \text{col}_{i=3,N}\{\Psi w_{i-1} - w_i - w_{i-2}\}$. The ML estimate of Ψ is the linear least squares estimate

$$\widehat{\Psi} = Y^{\#} Z \quad (6)$$

'#' designating the pseudo-inverse of Y. The frequency estimate $\widehat{f_0}$ is simply deduced by inverting eq. (4).
Given an estimate for f_0, we can now compute the two other parameters (amplitude and initial phase) in a same manner. Designating by $\Theta = (a\cos\phi, a\sin\phi)'$ the unknown vector of parameters, and expanding eq. (2)

$$\widehat{\Theta} = H^{\#} Y \quad (7)$$

with $H = \text{col}_{i=1,N}(\sin 2\pi\widehat{f}_0 t_i, \cos 2\pi\widehat{f}_0 t_i)$, a $N\times 2$ measurement matrix. So, inverting each component of $\widehat{\Theta}$ gives us the missing parameters: the amplitude and the initial phase of the sinusoid. At last, this 2-stage linear regression initiates a non-linear regression giving simultaneously the three parameters

$$(\widehat{f_0, a, \phi}) = \arg\min_{f_0,a,\phi} \sum_{i=0}^{N-1} (y_i - a\sin(2\pi f_0 iT + \phi))^2 \quad (8)$$

this problem is solved by a Gauss-Newton like algorithms with analytical Jacobian matrix. The entire process is repeated each sample time, where the window length N is taken lower than the minimum relative delay between successive paths to be sure that only one replica is present.

Step 2: jump detection The previous estimator performs correctly if there is a unique sinusoid in the window. In the case where 2 sinusoids are present (one pulse replica is ending, the other is beginning), the model is wrong. So, this mismodeling is used to detect the arrival of a new path. The jump detection test [4] is based on the sequence of backward/forward residuals for each sample time t

$$|z_1 - z_2| \lessgtr \eta \quad (9)$$

$$z_1 = \widehat{a}_1 \exp(j2\pi\widehat{f}_{01}t + \widehat{\phi}_1) \quad (10)$$

$$z_2 = \widehat{a}_2 \exp(j2\pi\widehat{f}_{02}t + \widehat{\phi}_2) \quad (11)$$

η being a threshold to decide whether one or two sinusoids are present. Subscripts 1 and 2 designate the backward and forward windows (surrounding current time t), and label the corresponding estimates.

Step 3: pulse duration The basic idea to estimate the duration of the pulse is to autocorrelate the residual error coming from the jump detection test. Then the position of the second maximum will give the pulse duration, and the identification of the beginning and ending times for each path allows to estimate the relative time–delays.

Step 4: range–depth location Step 3 delivers measurements of time–delays for each pulse replicas. The problem is now to fit these measurements τ_l^m with a model $\tau_l(R,z)$ derived from the SSP, ownship depth, and source location. Again the solution is obtained by minimizing the NL least-squares criterion below

$$(\widehat{R,z}) = \arg\min_{R,z} \sum_{l=1}^{M} \frac{(\tau_l^m - \tau_l(R,z))^2}{\sigma_\tau^2} \quad (12)$$

which is achieved by a Gauss–Newton algorithm after a coarse grid search initialization.

3 SIMULATION RESULTS AND PERFORMANCE

Let us consider the case of a bilinear sound speed profile and a source at range $R = 20$ km and depth $z = 80$ m, ownship depth being 90 m. Sampling rate is 1500 Hz, the frequency of the pulse is $f_0 = 400$ Hz, and its duration 0.5 s. Five ray paths are simulated according to the SSP: 2 refracted paths and 3 bottom reflected paths, yielding 4 possible time-delay measurements. The performance of the localization method is assessed by the comparison between empirical standard deviations of the range and depth estimates and the corresponding Cramer–Rao lower bounds (CRB). These CRB are made analytically computable due to a formalism introduced in [5] for the propagation aspects and [6, 7] for the localization part. For a 50 Monte–Carlo simulation and three different signal-to-noise ratios (SNR), the two tables below sum up the results in term of performance. The SNR definition is the following: $\frac{a^2T}{N_0}$, N_0 is the power spectral density of the noise, a the amplitude of the sinusoid, and T the duration of the pulse. Table 1 below concerns the range parameter and compares the mean and standard deviation of the range estimation to the true range value and the range CRB. Table 2 does the same for the source depth. Note that for the lowest SNR, only 27 trials have been declared convergent (time–delays are measurable), and also that due to the noisy estimation of the empirical standard deviations, $\widehat{\sigma_R}$ or $\widehat{\sigma_z}$ could be just beneath the CRB (it is the case for SNR=45 dB).

SNR(dB)	$\hat{R}$ (m)	$\widehat{\sigma_R}$ (m)	σ_R (m)
55	19994	14.8	10.8
45	19992	24.5	27.2
35	18728	1380	437

Table 1: range accuracy

SNR(dB)	$\hat{z}$ (m)	$\widehat{\sigma_z}$ (m)	σ_z (m)
55	78.3	3.0	2.1
45	78.6	4.3	5.0
35	155	74.2	8.6

Table 2: depth accuracy

4 AT–SEA EXPERIMENT

The experiment consists in a 1-hour recording of signals. The target is going South at speed 4.5 kts, whereas the receiving sonar has heading 320 deg and speed 12 kts. Azimuth is measured by the sonar from a conventional beamformer, in order to plot the estimation of the source location in cartesian axes. Target and ownship depths are respectively 80 and 90 m. The SSP is a summer Mediterranean profile that is a quasi bilinear function of the depth. Both emitter and receiver are below the SOFAR duct ($\approx$ 50 m) insuring a good propagation of the SOFAR rays.

A set of 26 pulses was detected by the sonar during the experiment. An example of sinusoid parameter estimation and jump detections is displayed on Fig.3 : the SOFAR paths are too close to be separated (a "mean" path gives the beginning of the pulse), but two SRBR1 paths are detected (so their relative time-delays to the SOFAR ray).

The result of the global localization process is displayed on Fig.3 : the use of a constant SSP exhibits a range bias of about+50%, whereas a bilinear SSP induces quite no bias and provides satisfactory results in comparison with the true motion of the target. The reason is that the main SOFAR rays are bottom refracted paths which are bent downwards, so the travel time difference between SOFAR and rectilinear paths is large.

5 CONCLUSION

A non–linear regression based algorithm in conjunction with a jump detector working on backward/forward linear prediction residuals has been developed to estimate the 3 parameters of overlapping CW pulses. Monte–Carlo simulations have demonstrated the efficiency of the method up to 35 dB in a bin. An experiment in the deep Mediterranean channel has also proved the interest of using a rather good approximation of the sound speed profile (bilinear instead of constant) in order to have an unbiased source range estimate.

Acknowledgment

This work was partly supported by GERDSM (Le Brusc – DCN Toulon, France).

References

[1] T.G. Manickam, R.J. Vacarro, and D.W. Tufts, "A Least-Squares Algorithm for Multipath Time-Delay Estimation", *IEEE trans. on Signal Processing*, Vol. 42, No. 11, 3229-3233, Nov. 1994

[2] R.J. Urick, "Principles of Underwater Sound", McGraw–Hill, NY, 1975.

[3] S.M. Kay, "Modern Spectral Estimation: Theory and Application", Prentice Hall, 1988.

[4] M. Basseville, and A. Benveniste, "Design and comparative study of some sequential jump detection algorithms for digital signals", *IEEE Trans on Acoust. Speech and Signal Proc.*, Vol. 31, No. 3, 521-535, 1983

[5] R.N. Baer, and M.J. Jacobson, "Sound transmission in a channel with bilinear sound speed and environmental variations", *J. Acoust. Soc. Am.* 54, 80-91 (1973).

[6] B. Friedlander, "Accuracy of source location using multipath delays", *IEEE trans. on Aerosp. Electron. Syst.*, vol. 24 no. 4, 346-359 (1988).

[7] P. Blanc–Benon, and G. Bienvenu, "Passive Target Motion Analysis using multipath differential time-delay and differential doppler shifts", in *Proc. of ICASSP'95*, Detroit, MI, (May 1995).

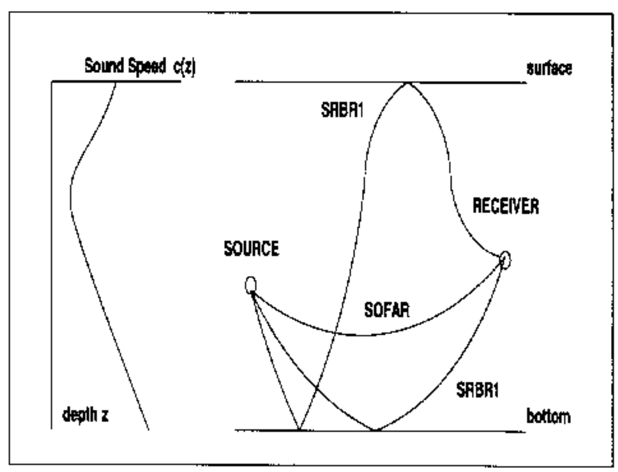

Figure 1: Mediterranean bathythermic conditions and related multipath

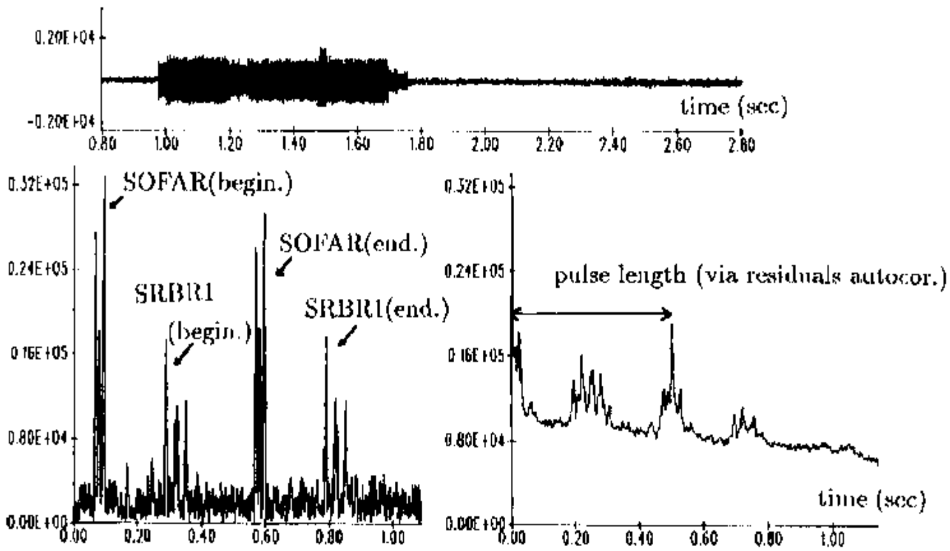

Figure 2: received CW pulse (top) for f_0=400Hz and sampling frequency 1500 Hz (pulse duration 0.5 sec), jump detection (bottom) via non-linear estimation exhibits both SOFAR (ie. the duct channel) and SRBR1 rays (ie. a single bottom reflection).

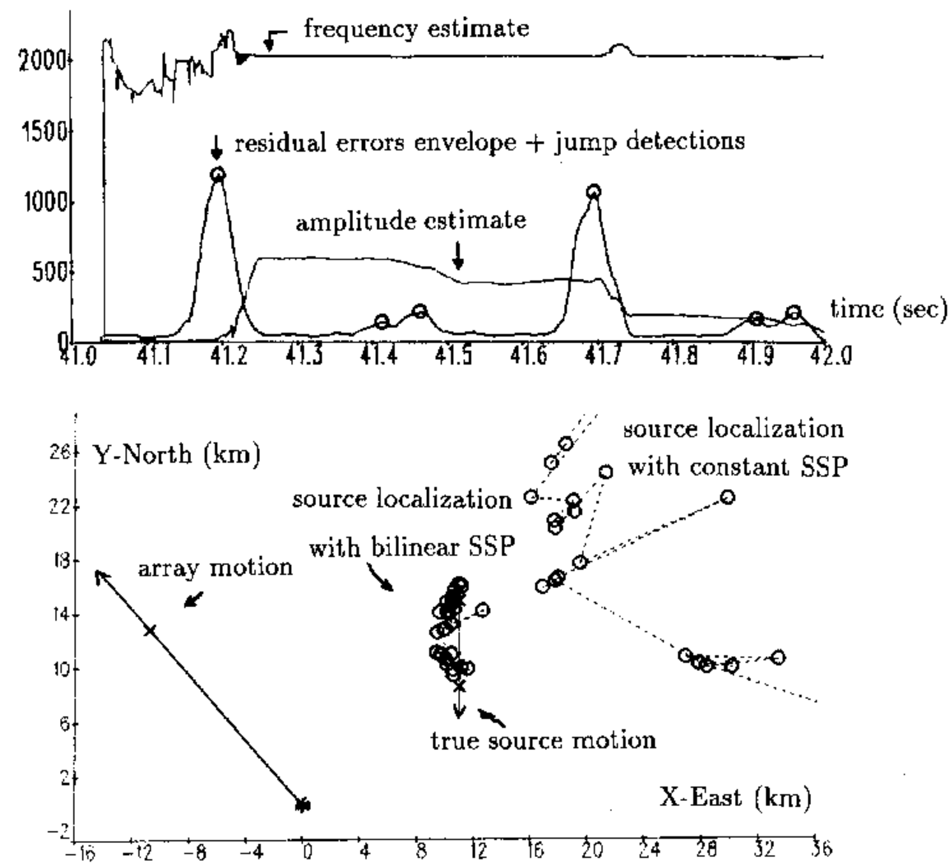

Figure 3: At-sea CW pulse parameter estimates (top) and source localization for constant SSP and bilinear SSP (bottom).